JCTC Journal of Chemical Theory and Computation

Location of Two Seams in the Proximity of the C_{2v} $\pi\pi^*$ Minimum Energy Path of Formaldehyde

Luca De Vico* and Roland Lindh

Department of Theoretical Chemistry, Lund University, P.O. Box 124, SE-22100 Lund, Sweden

Received August 22, 2008

Abstract: Photochemical reactions rationalization is a key aspect for the understanding and setup of novel experiment and novel photoinitiated pathways. In this respect, the relationship between minimum energy paths over an excited-state and the intersection to lower potential energy surfaces is fundamental. In order to help the understanding of this relationship, in this study we present a novel kind of constraint for geometry optimizations, namely, an "orthogonality" constraint. Its possible applications are described. A complete example on how to retrieve the direct relationship between a minimum energy path over an excited-state potential energy surface and a conical intersection seam is given for C_{2v} symmetry constrained formaldehyde. The advantages of using the novel constraint when rationalizing a (photo)chemical reaction are presented.

Introduction

Since Teller demonstrated the possibility for the existence of crossings of potential energy surfaces,[1] the interest for such entities increased, with an exponential trend in the latest years.[2] The available computational tools, coupled with the increasing capabilities of computers, turned the search for potential energy surface (PES) degeneracy points into an everyday matter,[3] making it indispensable when one wants to describe any photochemical reaction from the theoretical chemist point of view. Formally, the crossing between two potential energy surfaces of different spin symmetry is called intersystem crossing (ISC), while if the two surfaces share the same spin symmetry, the crossing is referred to as a conical intersection (CI).[4] Nevertheless, when considering molecules with symmetry, the crossing of two surfaces of the same spin belonging to different spatial symmetry can be treated in the same way as an ISC.

The nature of CIs (ISCs) has been extensively studied, by analyzing the PES around them. For example, Atchity and co-workers gave a classification of conical intersections based on the shape of the PES forming the CI.[5] On the base of which class a CI belongs to, they predicted different behaviors for the molecules passing through it and consequently for the photoreaction in general. Another aspect of crossings is their extension in the molecular coordinate space. In fact, there does not exist only one point of degeneracy but an infinite series.[6] This is usually referred to as intersection space[5] or intersection seam.[7] The nature of the points belonging to a seam has been recently studied by Sicilia and co-workers.[8] They analyzed the second-order nature of conical intersections and defined if they were minima or transition states inside the intersection space. Through this analysis, the authors were able to give a description of the CI seam and its main features. Very recently,[9] the same authors suggested an algorithm to connect the stationary points inside the intersection space.

Maybe more relevant for the study of a photochemical reaction is the relationship between the minimum energy paths (MEPs) over an excited-state PES and the seam connecting such a surface to other(s). To our knowledge, not too many studies have been conducted in this sense. Various attempts in this direction have been done, for example by locating the nearest crossing to a given structure, usually the Franck−Condon.[10,11] To name a few other examples related to different classes of molecules where the seam has been studied in more details, ref 12 reports a CI seam involved in the photochemistry of the ring-opening of cyclohexa-1,3-diene. Migani and co-workers analyzed the

* Corresponding author e-mail: luca@kemi.ku.dk. Current address: Department of Chemistry, University of Copenhagen, Universitetsparken 5, DK-2100 Copenhagen, Denmark.

10.1021/ct800348s CCC: $40.75
Published on Web 12/08/2008

CI seams of various models of the retinal chromophore.[13] Cembran et al. reported an extensive area of degeneracy for azobenzene,[14] while Frutos et al. described the involvement of CI seams in the photochemistry of tricyclo[3.3.0.0^{2,6}]octa-3,7-diene.[15] The knowledge of the relationship between a MEP and a CI seam has been, most interestingly, related also to the possibility of fine controlling the outcome of a photoreaction.[16] In fact, by knowing which internal modes correlate the MEP and the seam, one could define which vibrational levels should be pre-emptively excited in order to populate such modes. In turn, a coherent femtosecond pulsed laser experiment could be devised, in order to obtain the maximum yield of a desired photoproduct.[17]

The previously cited theoretical articles have one feature in common: the seam has been retrieved once the minimum energy crossing point (MECP) has been found or if a point along the MEP is also a crossing point. Starting from this structure, the rest of the seam is conceived. In a second moment, the seam and the MEP are put in energetic relation between each other. In other words, the relationship seam – MEP is partial (only energetic data are considered) and indirect. We devised a way to correlate a minimum energy path computed on an excited-state to the closest crossing that could be reached by vibrations along modes other than those involved in the MEP itself, in other words, along those modes perpendicular to the motion along the MEP. Since the MEP is defined as the steepest descend path, that is by the gradient, the crossing has to be located in the subspace of coordinates orthogonal to the gradient vector. In this way, the relationship seam – MEP is direct and easier to be rationalized. This is achieved because each point of the MEP is directly related to the points of the seam, in a one-to-one manner.

In the next paragraphs, we will give some more details on how this has been achieved, plus an application of the method to C_{2v} symmetry constrained formaldehyde on its evolution along the $\pi\pi^*$ excited state, together with related discussion.

2. Method

The methods section is divided into five parts: in the first we will sketch the theory behind the new kind of constraint we introduced, followed by a general discussion about its possible applications and its implementation. Finally, we will give the computational details of the application of the new kind of constraint to the search of a CI seam close to the C_{2v} $\pi\pi^*$ MEP of formaldehyde.

2.1. A New Type of Constraint: Theory. A new kind of constraint has been introduced and applied, an "orthogonality" constraint. Given a point in the coordinate space of a molecule (structure) and a vector associated to it (typically the energy gradient), the coordinate space available during a geometry optimization is reduced by the constraint to the subspace of coordinates orthogonal to the vector.

The constraint to fulfill can be expressed as

$$\langle \boldsymbol{g} \cdot (\boldsymbol{r_0} - \boldsymbol{r}) \rangle = 0 \qquad (1)$$

where $\boldsymbol{g}$ is the reference vector (gradient), $\boldsymbol{r_0}$ is the reference coordinates, and $\boldsymbol{r}$ is the coordinates of the current structure.

Scheme 1

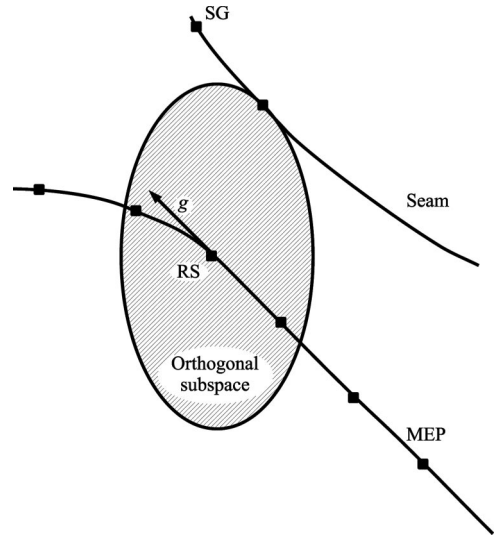

This kind of constraint is nearly useless when applied alone. In fact, in a typical situation, the reference vector is the gradient computed at the reference geometry $\boldsymbol{g} = \boldsymbol{g}(\boldsymbol{r_0})$. Once the orthogonality constraint is applied, the result of a constrained optimization would be the same reference geometry, since it is a minimum in the orthogonal subspace too. In fact, the only possibility to reach a structure with lower energy would be to follow the gradient, which has been cut out by the constraint. Once the geometry reaches the reference structure, the constraint vanishes, since one has $\boldsymbol{r} = \boldsymbol{r_0}$ in eq 1.

In an ideal situation, if the reference structure is a stationary point (minimum or transition state), the orthogonality constraint is noneffective. In fact, the reference gradient would be zero by definition ($\boldsymbol{g}(\boldsymbol{r_{eq}}) = 0$ in eq 1). The other eventual applied constraints would be the only effective.

2.2. Current Application to Photoreactions. The most interesting use, instead, is when the orthogonality constraint is coupled together with some other kind of constraint. This will induce $\boldsymbol{r} \neq \boldsymbol{r_0}$, making eq 1 meaningful. For example, in the present contribution, we coupled the orthogonality constraint together with the energy difference constraint. By doing so, we searched for the lowest energy degeneracy between two given potential energy surfaces inside the subspace orthogonal to the gradient computed at a given geometry. The obtained structure is not the absolute MECP but the lowest in energy and possibly closest crossing to the reference structure or to the starting geometry (*vide infra*). This is depicted in Scheme 1.

As for the hyperspherical constraint,[10] it is possible to specify a starting geometry and a reference structure/vector relative to another structure previously determined. For example, this has been applied in the present contribution to locate an intersection seam in the proximity of a previously computed MEP. In fact, the starting geometry (**SG**) was chosen to be already part of the seam that we wanted to explore. This, in turn, ensured continuity in the obtained seam. The gradient vector ($\boldsymbol{g}$) and the reference structure (**RS**), instead, were those of the MEP structure for which

Scheme 2

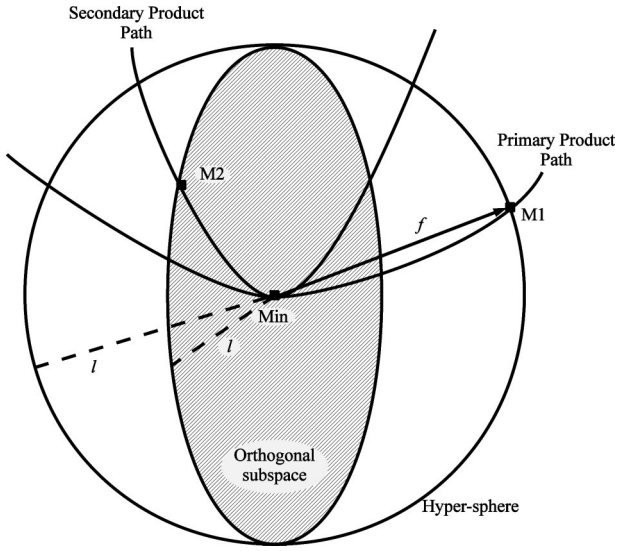

we were looking for the closest crossing point. More details on this procedure will be given in section 3.1.

2.3. Possible Applications to Thermal Reactions. Another possible usage of the orthogonality constraint is to find additional pathways leaving from a minimum. This, in turn, would help in locating secondary paths in, for example, thermal reactions. This usage has not been exploited in the present contribution, so it will be shortly described here. The procedure is depicted in Scheme 2. All minimizations described in this section are supposed to be fully successful.

Once a minimum structure (**Min**) has been optimized, it is possible to locate the first structure of a path (**M1**) leading away from it, by employing a normal hyperspherical constraint. That is, the only applied constraint is that **M1** is at a given distance l from **Min**. In this way, the structure with the lowest energy at the distance l from **Min** is found. In other words, given that the constrained optimization is successful, **M1** is the global minimum with respect to the hypersphere of radius l around **Min**.

One can define the vector between the two structures as the difference between the coordinates: $\boldsymbol{f} = Coord_{M1} - Coord_{Min}$. It is possible to start from **Min** another hyperspherical search with the same radius l and employing the additional constraint of being performed in the subspace orthogonal to $\boldsymbol{f}$. The so-found structure (**M2**) will be at higher energy than **M1**, but still a local minimum on the hyperspere. In other words, the two subsequent optimizations on the same hypersphere of radius l yields two different minima: the lowest in energy **M1** and the second to lowest **M2**.

In our view, **M2** represents the first point along a path that would lead from **Min** to a secondary reaction product. In principle, it is possible to define another vector $\boldsymbol{f}'$ as the difference between the coordinates of **M2** and **Min**. A subsequent hyperspherical search from **Min** in the subspace orthogonal to both $\boldsymbol{f}$ and $\boldsymbol{f}'$ would find a third local minimum, and so on. This procedure could be applied as long as the studied molecule has available degrees of freedom.

2.4. Implementation. The orthogonality constraint has been implemented in the MOLCAS code,[18] to be used in the same way as the other implemented constraints, through the usage of Lagrangian multipliers.[10] Our implementation[10] follows that of Anglada and Bofill[19] for constrained optimizations, in combination with the Rational Function approach[20] and no line-search techniques. In this approach the coordinate space is divided into two parts, one with dimensionality m where the constraint is fulfilled, and one of $3N-6(5)-m$ dimensions where an energy minimization is conducted (N being the number of atoms). In the first subspace the minimization is simply linear, according to eq 8 in ref 10. There is no need for an analytic Hessian evaluation. In the second subspace, the method makes use of the Broyden Fletcher Goldfarb Shanno (BFGS)[21] method for updating the approximate Hessian matrix. All the described optimization procedures require the evaluation of only first derivatives of the energy with respect to the spatial coordinates.

2.5. Computational Details. All calculations were performed in C_{2v} symmetry using a triple-ζ ANO-RCC basis set[22] with contraction scheme [4s3p2d1f] for C and O, [3s2p1d] for H. Energies and analytical gradients were computed at the state average (SA) complete active space multiconfigurational self-consistent field (CASSCF)[23] level of theory. The computed roots were as follows: the first two roots of symmetry $^1A_1$ (S_0 and $\pi\pi^*$) and the first root of symmetry $^1B_1$ ($\sigma\pi^*$). The active space comprised 6 electrons in 5 orbitals (6-in-5). The orbitals were chosen as the C-O π, π^*, σ, and σ^*, plus the O lone pair perpendicular to the π system. All minimum energy path (MEP) and conical intersection (CI) optimizations were performed as constrained optimization, using Lagrangian multipliers, as described in ref 10. All calculations were performed using the MOLCAS[18,24] version 7.1 suite of programs for quantum chemistry.

3. Results and Discussion

3.1. MEP and Seams Construction. The coordinates and CASSCF energies of all the computed geometries are reported in Tables 2 and 3, respectively, in the Supporting Information. The formaldehyde structure was fully optimized on the S_0 state. Such geometry was used as a starting point (Franck−Condon structure, **FC**) for a subsequent MEP search in the $\pi\pi^*$ state. The used step was 0.05 au (in mass-renormalized mass-weighted coordinates).[25] The MEP search was stopped as soon as a minimum was located (**Min** $\boldsymbol{\pi\pi^*}$). The MEP is reported in Figure 1 as a red continuous line. For each MEP point, the S_0 (light blue dot-dashed line in Figure 4 in the Supporting Information) and $\sigma\pi^*$ (dashed green line in Figure 1) energies were computed. A conical intersection between the $\pi\pi^*$ and the $\sigma\pi^*$ potential energy surfaces (PESs) was also located as a minimum energy crossing point. This **MECP** was found to lie close to the MEP structure **MEP6** that lies 0.3 au from **FC**.

Using as reference the **FC** structure and its energy gradient vector as computed on the $\pi\pi^*$ PES, another conical intersection was searched, employing the additional orthogonality constraint. This structure (**SA0**), even if it has nearly the same energy as the $\pi\pi^*$ state energy of **FC**, presents a

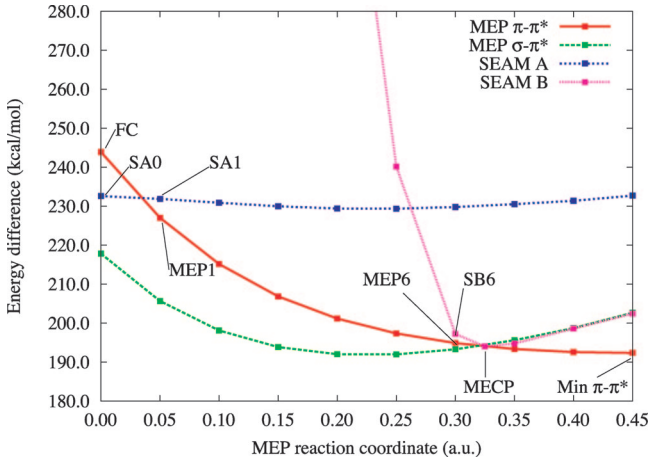

Figure 1. MEP - seam energy relation. For the MEP points, both $\pi\pi^*$ and $\sigma\pi^*$ energies are reported. Along the seams these two potential energy surfaces are degenerate. Energies computed as relative to the S_0 energy of FC, in kcal/mol. Reaction coordinate in mass-renormalized mass-weighted a.u. The complete SEAM B is reported in Figure 4 in the Supporting Information.

Table 1. Geometrical Data (Distances in Ångstroms, Angles in Degrees) for the Notable Structures Discussed in the Text

structure	O-C	C-H	O-C-H
Min S_0 **FC**	1.215	1.082	121.2
Min $\pi\pi^*$	1.631	1.065	118.9
MECP	1.561	1.060	114.9
SA0	1.810	1.059	74.5
SB0	1.337	0.468	144.5

quite distorted geometry. See Table 1. **SA0** is around 0.7 au far from **FC**.

SA0 was used as the starting structure to locate the rest of SEAM A, in an iterative way. In fact, **SA1** was located via a constrained optimization, where the constraints were the $\pi\pi^*$ and $\sigma\pi^*$ energies difference and the condition of orthogonality to **MEP1**, the first MEP point after **FC**, as depicted in Scheme 1. In other words, **MEP1** was used as **RS** and the gradient as ***g*** vector. **SA0** was, instead, the **SG**. The geometry of **SA1** was used as the starting geometry to locate **SA2** in a similar manner and so on for the rest of the SEAM A points. In this way, continuity of the seam was ensured. The results are presented in Figures 1 and 2 as a dotted dark blue line.

As can be seen in Figure 2, SEAM A is never closer than 0.5 au to the computed MEP. On the other hand, **MECP** was found to be quite close to the MEP (less than 0.05 au). We decided to search for an alternative seam, using **MECP** as **SG** and **MEP6** for reference, both structure and gradient vector. In this way we located another crossing point not part of SEAM A. We named this structure **SB6**. Using the geometry of **SB6** as the starting structure, we located the other points of SEAM B iteratively, as before, as relative to the entire MEP structures. These are reported in Figures 1 and 2 as a dotted violet line.

3.2. Seams Comparison. As can be clearly seen from Figures 1 and 2, the two seams are quite different from each other. As previously mentioned, SEAM A is almost always

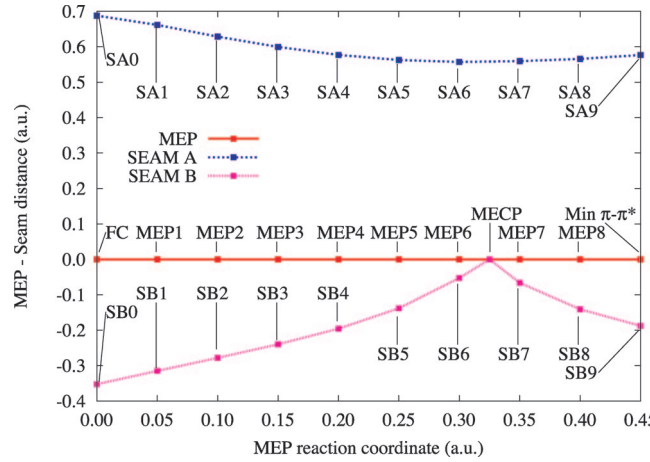

Figure 2. MEP - seam distance relation, in mass-renormalized mass-weighted au.

at the same energy (Figure 1) but is never close to the MEP (Figure 2). The situation is quite the opposite for SEAM B. The seam starts quite high in energy (Figure 4 in the Supporting Information) but gets very close to the MEP (Figure 2) before slowly getting far from it again. Notably, SEAM A is always lower in energy than the $\pi\pi^*$ energy of **FC**, while SEAM B goes under this value only in close proximity to **MECP**. On the other hand, after **FC** SEAM A is always higher in energy than the MEP.

3.3. MEP - Seam Relation. The differences of the two seams make them differently accessible. In fact, by simply following the MEP, SEAM B would be accessed only when the MEP reaches the proximity of **MECP**. This motion requires some stretching of the C═O bond. To access SEAM B otherwise earlier, a certain quantity of extra vibrational energy is needed.

Since it is always far from the MEP, also SEAM A cannot be accessed unless some vibrational energy is spent. Figure 3 shows the different structural changes to access **SA0** or **SB0** from **FC**. If **FC** would possess enough vibrational energy along its CH_2 scissoring mode, the molecule would then access SEAM A. If, instead, it would possess enough vibrational energy along its CH_2 symmetric stretching mode, it will access SEAM B. Since the two modes, CH_2 scissoring and stretching, have different and well separated absorption peaks (ca. 2782 and ca. 1500 cm^{-1} respectively),[26] it should be possible to direct the decay toward one of the seams. If, otherwise, the most populated vibrational mode would be the C═O stretching (ca. 1746 cm^{-1}),[26] then the molecule would follow preferably the MEP and decay at **MECP**.

Obviously, apart from the vibrational mode, also the quantity of vibrational energy is important. As evident from Figure 1, in order to reach SEAM A is necessary less (no) energy than to reach the first part of SEAM B. A higher level computational method taking in consideration full electron correlation like (MS-)CASPT2,[27] would then be needed for a more quantitative evaluation of the amount of vibrational energy needed.

3.4. Photoreaction Rationalization. Through the analysis of the direct relationship between the computed MEP and seams, it is possible to rationalize the photoreaction of formaldehyde.

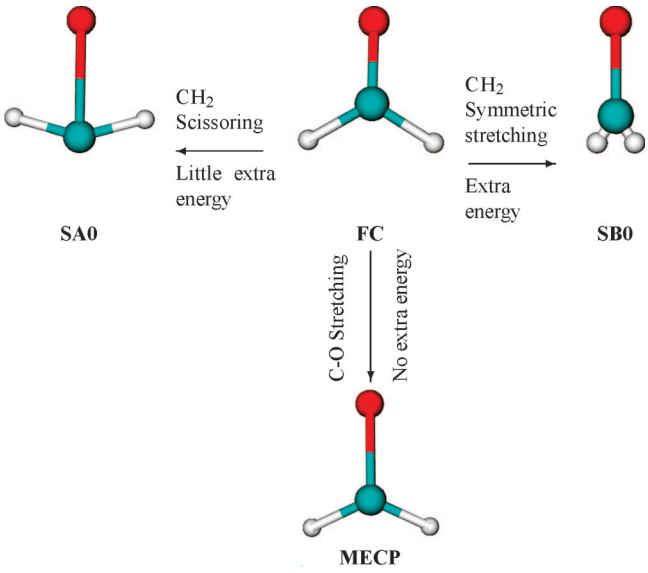

Figure 3. Structures of **FC**, **SA0**, **SB0**, and **MECP**. Indicated the relative vibrational modes, of A_1 symmetry, involved when the molecule exits **FC**. Also, a qualitative indication of the amount of energy needed to reach each structure is reported.

After the photoexcitation, depending on which vibrational mode is active, it is possible to indicate three possible fates for the molecule. For the purposes of this study, this analysis is only qualitative, since the energetic data are based on CASSCF results and not on a more accurate method, as previously mentioned. This is depicted also in Figure 3.

(i) If formaldehyde is vibrationally excited along its C═O stretching mode, it will follow the MEP, and decay on the lower state at **MECP** or in close proximity to it. No vibrational energy is strictly needed to access **MECP**, since it is part of the MEP.

(ii) When the CH_2 scissoring mode is active, the molecule has a high chance of reaching SEAM A, since it is nearly at the same energy as **FC**.

(iii) If the CH_2 symmetric stretching mode is populated with sufficient energy, it is possible for the molecule to decay through SEAM B earlier than MECP.

Obviously, the amount of energy needed to reach **SA0** or **SB0** should take into consideration also the eventual presence of a barrier. However, in the proximity of the MEP it is expected that the potential energy surface, in the direction perpendicular to the MEP, is harmonic, i.e. no energy barrier to reach the seam is expected.

The general methodology we described can be applied to any kind of photoreaction. We would like to stress the importance such an analysis might have with the following example. One could consider the situation reported in Scheme 3, similar to what was reported in Figure 2. Along the MEP of Scheme 3, a MECP has been found. The usual methodologies would use this structure as a starting point to explore and characterize SEAM Y. It is possible, although, that this would not find SEAM X. If SEAM X would be energetically accessible from the MEP, then not including it would cause serious mistakes. For example, by considering only the relationship between the MEP and SEAM Y, one might draw

Scheme 3

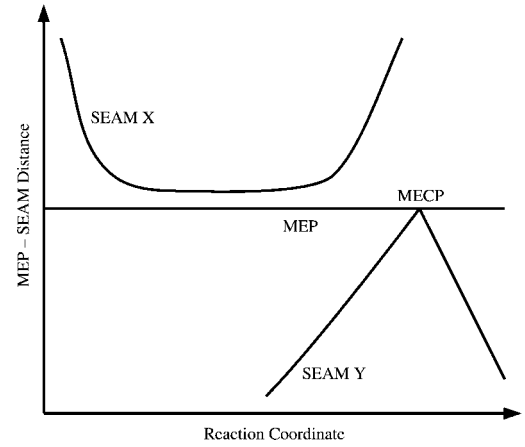

some erroneous conclusions about the decaying rate of the excited molecule. Moreover, if the photoproducts of SEAM X and SEAM Y would be different, the photoproduct of SEAM X would be totally ignored. With our approach, instead, SEAM X would be immediately found, as happened with formaldehyde. Starting then from MECP, also SEAM Y would be located.

If the molecule would possess enough degrees of freedom, additional seams could be searched. Let us consider a point of the MEP, for example the tenth, MEP10. By the previous analysis, the corresponding seam points SX10 and SY10 belonging to SEAM X and Y, respectively, have been found. It is possible to compute the geometry difference vectors $\boldsymbol{f} = Coord_{SX10} - Coord_{MEP10}$ and $\boldsymbol{f}' = Coord_{SY10} - Coord_{MEP10}$. For each of the vectors g (the gradient of MEP10), $\boldsymbol{f}$ and $\boldsymbol{f}'$, one orthogonality constraint is applied. A subsequent optimization of an energy difference structure would locate a point belonging to a third different seam, SEAM Z. This procedure could be carried on for as long as there are available degrees of freedom. In practice, of course, the energy difference between the MEP and the seam should indicate when it is not meaningful anymore to search for additional seams.

4. Conclusions

In this study we presented a novel kind of constraint, namely a orthogonality constraint. We demonstrated how the usage of this constraint in conjunction with the one to minimize the energy difference between two potential energy surfaces can be successfully used to describe conical intersection seams, in relationship to excited-state minimum energy paths. In particular, we showed how to locate two different seams in the proximity of the C_{2v} $\pi\pi^*$ minimum energy path of formaldehyde. The direct relation seam - MEP permitted the easy rationalization of the normal modes possibly involved in the photoreaction.

As previously mentioned, the orthogonality constraint requires only first derivatives of the energy with respect to the spatial coordinates. This fact permitted us to explore a seam without the further need of an analytical Hessian. An approximative Hessian in association with the BFGS update method is, in fact, sufficient.

As an outlook, we are currently studying how to implement an explicit vibrational analysis of the reduced Hessian along the MEP. In other words, for each of the retrieved MEP points, a vibrational analysis should be performed on all molecular modes except the gradient. Coupling this information with the knowledge of where the seam lies should give a complete as possible view of the photochemical event. Today, this can be achieved only through the use of the computationally very expensive molecular dynamics methods.

It is our hope that in the future our procedure will be applied to study how to enhance the quantum yields of desired photoproducts by the rational design of coherent femtosecond pulsed laser experiments. The application of our constraint in order to explore the paths leading to secondary products of thermal reaction is also highly expected. Also in this case, the geometries of the structures along the different paths should be analyzed in relationship with the vibrational modes of the fundamental state minimum. This, in turn, should provide a rational way to direct thermal reaction through excitation by specific infrared frequencies.

Acknowledgment. The authors thank LUNARC computer centre of Lund University and SNAC for granted computational time and the Swedish Scientific Research Council (VR). L.D.V. acknowledges a grant from the Foundation BLANCEFLOR Boncompagni-Ludovisi neé Bildt.

Supporting Information Available: Figure with the complete energetic of Figure 2 (Figure 4) and tables with the coordinates and relative energies of all computed structures (Tables 2 and 3). This material is available free of charge via the Internet at http://pubs.acs.org.

References

(1) Teller, E. *J. Phys. Chem.* **1937**, *41*, 109.

(2) Domke, W.; Yarkony, D. R.; Köppel, H. *Conical Intersections Electronic Structure, Dynamics & Spectroscopy*; World Scientific: Singapore, 2004.

(3) Olivucci, M. *Computational Photochemistry*; Elsevier: Amsterdam, 2005.

(4) Braslavsky, S. E. *Pure Appl. Chem.* **2007**, *79*, 293–465.

(5) Atchity, G. J.; Xantheas, S. S.; Ruedenberg, K. *J. Chem. Phys.* **1991**, *95*, 1862–1876.

(6) (a) Salem, L. *Electrons in Chemical Reactions: First Principles*; Wiley: New York, 1982. (b) Klessinger, M.; Michl, J. *Excited States and Photochemistry of Organic Molecules*; VCH Publishers: New York, 1995.

(7) Yarkony, D. R. *J. Phys. Chem. A* **2001**, *105*, 6277–6293.

(8) (a) Sicilia, F.; Blancafort, L.; Bearpark, M. J.; Robb, M. A. *J. Phys. Chem. A* **2007**, *111*, 2182–2192. (b) Sicilia, F.; Bearpark, M. J.; Blancafort, L.; Robb, M. A. *Theor. Chem. Acc.* **2007**, *118*, 241–251.

(9) Sicilia, F.; Blancafort, L.; Bearpark, M. J.; Robb, M. A. *J. Chem. Theory Comput.* **2008**, *4*, 257–266.

(10) De Vico, L.; Olivucci, M.; Lindh, R. *J. Chem. Theory Comput.* **2005**, *1*, 1029.

(11) Levine, B. G.; Coe, J. D.; Martínez, T. J. *J. Phys. Chem. B* **2008**, *112*, 405–413.

(12) Garavelli, M.; Page, C. S.; Celani, P.; Olivucci, M.; Schmid, W. E.; Trushin, S. A.; Fuss, W. *J. Phys. Chem. A* **2001**, *105*, 4458–4469.

(13) (a) Migani, A.; Robb, M. A.; Olivucci, M. *J. Am. Chem. Soc.* **2003**, *125*, 2804–2808. (b) Migani, A.; Sinicropi, A.; Ferré, N.; Cembran, A.; Garavelli, M.; Olivucci, M. *Faraday Discuss.* **2004**, *127*, 179–191.

(14) Cembran, A.; Bernardi, F.; Garavelli, M.; Gagliardi, L.; Orlandi, G. *J. Am. Chem. Soc.* **2004**, *126*, 3234–3243.

(15) Frutos, L. M.; Sancho, U.; Garavelli, M.; Olivucci, M.; Castano, O. *J. Phys Chem. A* **2007**, *111*, 2830–2838.

(16) Hunt, P. A.; Robb, M. A. *J. Am. Chem. Soc.* **2005**, *127*, 5720–5726.

(17) Dantus, M.; Lozovoy, V. V. *Chem. Rev.* **2004**, *104*, 1813–1859.

(18) Karlström, G.; Lindh, R.; Malmqvist, P.-Å.; Roos, B. O.; Ryde, U.; Veryazov, V.; Widmark, P.-O.; Cossi, M.; Schimmelpfennig, B.; Neogrady, P.; Seijo, L. *Comput. Mater. Sci.* **2003**, *28*, 222.

(19) Anglada, J. M.; Bofill, J. M. *J. Comput. Chem.* **1997**, *18*, 992–1003.

(20) Banerjee, A.; Adams, N.; Simons, J.; Shepard, R. *J. Phys. Chem.* **1985**, *89*, 52–57.

(21) (a) Broyden, C. G. *Math. Comput.* **1970**, *24*, 365–382. (b) Fletcher, R. *Comput. J.* **1970**, *13*, 317–322. (c) Goldfarb, D. *Math. Comput.* **1070**, *24*, 23–26. (d) Shanno, D. F. *Math. Comput.* **1970**, *24*, 647–656.

(22) Roos, B. O.; Lindh, R.; Malmqvist, P.-Å.; Veryazov, V.; Widmark, P.-O. *J. Phys. Chem. A* **2005**, *108*, 2851.

(23) Roos, B. O.; Taylor, P. R. *Chem. Phys.* **1980**, *48*, 157–173.

(24) Veryazov, V.; Widmark, P.-O.; Serrano-Andrés, L.; Lindh, R.; Roos, B. O. *Int. J. Quantum Chem.* **2004**, *100*, 626–635.

(25) The mass-weighted coordinates are divided by the square root of the total molecular mass. Hence, the mass-renormalized mass-weighted coordinates correspond to a length.

(26) Wohar, M. M.; Jagodzinski, P. W. *J. Mol. Spectrosc.* **1991**, *148*, 13–19.

(27) (a) Andersson, K.; Malmqvist, P.-Å.; Roos, B. O.; Sadlej, A. J.; Wolinski, K. *J. Phys. Chem.* **1990**, *94*, 5483. (b) Andersson, K.; Malmqvist, P.-Å.; Roos, B. O. *J. Chem. Phys.* **1992**, *96*, 1218. (c) Roos, B.; Andersson, K.; Fülscher, M.; Malmqvist, P.-Å.; Serrano-Andŕes, L.; Pierloot, K.; Merchán, M. Multiconfigurational perturbation theory: Applications in electronic spectroscopy In *Advances in Chemical Physics: New Methods in Computational Quantum Mechanics*; Prigogine, I.; Rice, S., Eds.; John Wiley & Sons: New York, 1996; pp 219−332.

CT800348S